HHS Public Access

Author manuscript

Leukemia. Author manuscript; available in PMC 2014 May 01.

Published in final edited form as:

Leukemia. 2013 November ; 27(11): 2209–2219. doi:10.1038/leu.2013.103.

p190-B RhoGAP regulates the functional composition of the mesenchymal microenvironment

Rachna Raman, **Rupali Sani Kumar**, **Ashwini Hinge**, **Sachin Kumar**, **Ramesh Nayak**, **Juying Xu**, **Kathleen Szczur**, **Jose A. Cancelas**, and **Marie-Dominique Filippi**[#]

Division of Experimental Hematology and Cancer Biology, Cincinnati Children's Research Foundation, University of Cincinnati College of Medicine, Cincinnati OH, USA

Abstract

Hematopoiesis is regulated by components of the microenvironment, so-called niche. Here, we show that p190-B GTPase Activating Protein (p190-B) deletion in mice causes hematopoietic failure during ontogeny, in p190-B$^{-/-}$ fetal liver and bones, and in p190-B$^{+/-}$ adult bones and spleen. These defects are non-cell autonomous, since we previously showed that transplantation of p190-B$^{-/-}$ hematopoietic cells into wild-type hosts leads to normal hematopoiesis. Coculture of mesenchymal stem/progenitor cells (MSC) and wild-type bone marrow cells reveals that p190-B$^{-/-}$ MSCs are dysfunctional in supporting hematopoiesis due to impaired Wnt signaling. Furthermore, p190-B loss causes alteration in bone marrow niche composition, including abnormal CFU-fibroblast, CFU-adipocyte and CFU-osteoblast numbers. This is due to altered MSC lineage fate specification to osteoblast and adipocyte lineages. Thus, p190-B organizes a functional mesenchymal/microenvironment for normal hematopoiesis during development.

Keywords

mesenchymal stem cell; p190-B RhoGAP; hematopoiesis; microenvironment; Wnt3a

Introduction

Hematopoiesis arises from the development of multipotent hematopoietic stem cells (HSCs) into mature blood cell lineages. HSCs also have the ability to regenerate themselves or “self-renew” in order to maintain an adequate number of both mature cells and HSCs. Life-long hematopoiesis warrants a balance between HSC quiescence, proliferation and

[#] Corresponding author Marie-Dominique Filippi, PhD Division of Experimental Hematology and Cancer Biology - S7.605 Cincinnati Children's Research Foundation, 3333 Burnet Av, Cincinnati, OH 45229 Phone: 513-636-0991 Fax: 513-636-3768 Marie-Dominique.Filippi@cchmc.org.

Author contributions

Rachna Raman designed and performed experiments, analyzed the data and wrote the paper; Rupali Sani Kumar and Ashwini Hinge designed and performed experiments, and analyzed the data; Sachin Kumar, Rames Nayak, Juying Xu, Kaltheen Szczur performed experiments; Jose A. Cancelas provided key advice in research design, data analysis and editing the paper; Marie-Dominique Filippi designed and directed the program research, analyzed data, and wrote and edited the manuscript.

Supplementary information is available at the journal's website

The authors declare no conflict of interest.

differentiation, which is tightly regulated by the hematopoietic stem and progenitor cell (HSC/P) microenvironment, so-called “niches”. [1-3] During embryogenesis, HSCs travel to various anatomical sites, ie AGM, fetal liver, fetal bones and adult bones, and likely are exposed to different types of microenvironment. [4] While the establishment and organization of hematopoietic niches remains to be defined in detail, several non-hematopoietic cells are critical for HSC functions, including osteoblasts (in bones), endothelial cells, and perivascular, mesenchymal, stromal cells, and adipocytes. Niche cells support hematopoiesis by secreting factors, such as stem cell factor, Angiopoeitin1, TPO, SDF-1α, Wnt, NOTCH, and Osteopontin, and by providing direct physical support through integrin/ligand interaction. [1-3]

Mesenchymal stem cells (MSCs) appear to have unique roles. They are self-renewing multipotent progenitors that can differentiate into various mesenchymal lineages, (at least bone, fat and cartilage) [5, 6]. MSCs can give rise to the majority of HSC niche constituents (including stromal cells, osteoblasts, adipocytes, chondrocytes), and, thus, in theory appears to be able to contribute to the establishment and organization of the niche. [7-9] They also directly interact with HSCs and support hematopoiesis by secreting cytokines [10]. The importance of niche components is illustrated by studies showing that dysregulation in the microenvironment can influence hematopoietic disease development. An abnormal microenvironment appears to contribute to the pathogenesis of inherited bone marrow failure, such as Fanconi anemia [11] or Shwachman-Diamond Syndrome. [12] Despite its importance, little is known about the molecular regulation of hematopoietic stem cell niche organization and functions.

Members of the Rho GTPase family (e.g. Rho, Rac, cdc42) operate as molecular switches that effect signaling downstream of numerous receptors and play a crucial role in cytoskeleton dynamics, cell migration, adhesion and cell-cycle progression [13]. They cycle between an active GTP-bound and an inactive GDP-bound state, which is regulated by guanine nucleotide exchange factors (GEFs) and GTPase activating proteins (GAPs) [14]. Rho activity modulates MSC differentiation inducing osteogenesis or adipogenesis [15], well known positive and negative regulators of hematopoiesis, respectively [16, 17]. p190-B RhoGAP (p190-B) is a negative regulator of RhoA activity [18]. Disruption of p190-B in gene-targeted mice has revealed defects in cell size, thymus and lung during fetal development. Interestingly, p190-B loss in embryonic mesenchymal/fibroblasts leads to an imbalance in adipogenesismyogenesis cell fate determination [19-21]. We previously reported the intrinsic role of p190-B in HSC functions and showed that loss of p190-B enhanced HSC self renewal ability, as seen by greater competitive repopulation activity of p190-B-deficient HSC than WT cells, during serial transplantation in WT animals [22]. Here, we provide evidence that p190-B is critical for the constitution of a functional mesenchymal-derived hematopoietic niche.

Materiel and Methods

Mice model

p190-B RhoGAP$^{+/-}$ mice (backcrossed into C57BL/6J N=10), and B6.SJLPtrcaPep3b/BoyJ (B6.BoyJ, CD45.1^{+}) congenic mice were bred in house in pathogen-free environment. All

studies were conducted with a protocol approved by the Animal Care Committee of Cincinnati Children's Hospital Medical Center.

In vitro culture of stromal cells

Stromal cells were derived from E14.5 p190-B−/− and WT fetal livers. The cells were cultured in Iscove's Modified Dulbecco's Medium (IMDM) containing 20% fetal bovine serum (FBS, Omega Scientific, Tarzana, CA) and beta mercaptoethanol (2-ME, Sigma Aldrich, St. Louis, MO). The adherent cells were grown to 70-80% confluence, passaged and sub-cultured in medium containing EGF (10ng/ml) and PDGF (20ng/ml) (Peprotech, Rocky Hill, NJ). The cells were depleted for CD11b using lineage depletion kit (Miltenyi biotec Inc, Auburn, CA) as per the manufacturer's protocol. All experiments were performed on primary stroma of early passages (p3-p7) and exhibiting similar immunophenotype between the genotypes.

Myeloid and erythroid colony forming unit (CFU) assay, were performed as previously described [22].

Flow cytometry analyses

Lineage staining utilized a cocktail of biotinylated anti-mouse antibodies to anti-CD11b (M1/70), anti-B220 (RA3-6B2), anti-CD5 (53-7.3), anti-Gr-1 (RB6-8C5), anti-Ter119, and anti-CD8a (53-6.7), and streptavidin-APC-Cy7 or Alexa Fluor 700. Directly conjugated antibodies were anti–Sca-1-PEcy7 (clone D7; eBioscience, San Diego, CA), anti–c-kit-APC or APC-Cy7 (clone 2B8), anti-CD48-FITC, anti-CD150-PE or APC (eBioscience, San Diego, CA), anti-Ter119-FITC, anti-CD71-PE, anti-CD45.1-PE and anti-CD45.2-FITC, anti-CD90-APC, anti-CD105-PE, anti-CD73-Alexa 405, anti-CD44-biotin and anti-CD31-FITC were used. Unless specified, all Abs were from BD Pharmingen, San Diego, CA. Fluorescence-activated cell analysis was performed with a Facscanto (Becton Dickinson, San Jose, CA)

Cocultures

Stromal cells and freshly isolated bone marrow cells or lineage-Sca1+c-Kit+ (LSK) cells were cocultured in CAFC conditions [23]. Stromal cells grown at 80-90% confluence were irradiated (10Gy) and cells were seeded on the irradiated stromas at various cell concentrations. Coculture were grown in CAFC medium (IMDM containing 20% horse serum (Omega),2-ME and hydrocortisone (Sigma Aldrich) (at 37°C, 5% CO_2) for 2 weeks. The wells containing cobblestone area were scored and the frequency of CAFC was calculated [23]. In addition, 1 week coculture was harvested and used for myeloid colony forming unit (CFU) assay or for competitive repopulation assay. In this experiment, one week coculture harvest was mixed with freshly isolated competitor BM cells (BoyJ; CD45.1, 2×10^5 cells) and transplanted into lethally irradiated BoyJ mice (CD45.1; 3 mice/group, 2 independent experiments). The peripheral blood was analyzed for the frequency of CD45.2 by flow cytometry. Finally, cocultures were performed with stroma and isolated LSK cells in presence or absence of rWnt3a (100ng/ml). CFU was carried out after 1 week.

CFU- fibroblast (CFU-F) assay

One million total fetal liver cells (e14.5) or 2000 cultured-derived stromal cells or one half of e18.5 femur were used in the assay. Briefly, the cells were seeded in methyl cellulose medium containing FBS, L-glutamine, penicillin, streptomycin and 100μM 2-ME. The assay was set in triplicate. The cells were incubated (at 37°C, 5% CO_2) for 14 days, then methyl-cellulose was washed, the adherent fibroblast colonies were fixed and stained with Diff-Quik stains (Siemens, Newark, USA) and the colonies were scored.

CFU-adipocyte

BM cells isolated from femur of e18.5 embryos using Bone Marrow Harvesting & Hematopoietic Stem cell Isolation Kit (Millipore, Billerica, MA) were cultured in methylcellulose medium containing 20% FBS, 100μM 2-ME, penicillin, streptomycin, L-Glutamine, 0.1μM dexamethasone (Sigma Aldrich), 50μM indomethacin (Sigma Aldrich) and 5μg/ml of insulin (Sigma Aldrich). The culture was incubated for four weeks (at 37°C, 5% CO_2) and adipocyte differentiation was assessed by Oil red O staining. The assay was set in duplicate.

CFU-osteoblast

BM cells isolated from femur of e18.5 embryos were cultured in methylcellulose medium containing 20% FBS, 100μM 2-ME, penicillin, streptomycin, 2mM LGlutamine, 10μM dexamethasone, 10mM beta glycerophosphate (Sigma Aldrich) and 25μM ascorbic acid (Sigma Aldrich). The culture was incubated for 2 weeks (at 37°C, 5% CO_2) and osteoblastic differentiation was assessed by alkaline phosphatase staining (alkaline phosphatase kit, Stemgent, Cambridge, MA, USA). The assay was set in duplicate.

Differentiation of stromal cells

Adipocytic—The cells were grown in DMEM medium containing 10% FBS, dexamethasone (100μM), insulin (500ng/ml) and indomethacin (60μM). Fresh medium was added after every 72 hours. The cells were maintained in culture for 14 days. They were either fixed and stained with adipocytic specific Oil red O stain by Lillie and Ashburin's method or used for qPCR analyses using specific primers for C/EBP alpha and PPAR gamma. The assay was set in duplicate.

Osteoblastic—The cells were grown in DMEM medium containing 20% FBS, dexamethasone (10μM), beta glycerophosphate (10mM) and ascorbic acid (25μM) for 12 days. The cells were either fixed or stained for alkaline phosphatase staining or used for qPCR analyses using specific primers for alkaline phosphatase, Runx2 and osteocalcin. The assay was set in duplicate.

qPCR analyses

RNA isolation and cDNA preparation were performed as per manufacture's protocol (RNeasy micro kit, Quiagen, Superscipt III system, Invitrogen). The cDNA was amplified by real time PCR using SYBR green master mix (SA bioscience) and specific primers (see primer sequence in supplemental table 1). Beta actin was used as an internal control.

Bone marrow histology was performed at the Pathology Laboratories at CCHMC. Sections were stained with hematoxylin and eosin or Masson's trichrome staining, as indicated in figure legends.

Statistical analysis

Data are expressed as Mean± SD. Differences in the group were analyzed using unpaired T test (2 tailed). Differences in mRNA expression assessed by qPCR analysis were analyzed using Mann-Whitney test (2 tailed). P values <0.05 were considered as significant.

Results

p190-B$^{-/-}$ fetal hematopoiesis is defective despite increased HSC self-renewal

Mice lacking p190-B die at birth [20]. We previously reported that p190-B$^{-/-}$ HSCs derived from embryonic day 14.5 post coitum (e14.5) fetal livers have enhanced self renewal ability relative to their WT counterparts, in serial competitive transplantation assay. In addition, p190-B$^{-/-}$ HSCs retain normal multilineage differentiation potential in non-competitive transplantation assay. Intriguingly, e14.5 p190-B$^{-/-}$ embryos exhibited signs of hematopoietic defects with a 2-fold decrease in numbers of myeloid progenitors (ie, CFU-GM, BFU-E and CFU-mix) per liver [22], suggesting the existence of additional functions for p190-B. We thus systematically explored hematopoiesis in p190-B$^{-/-}$ animals. E14.5 and e15.5 p190-B$^{-/-}$ embryos appeared paler than WT littermates (Figure 1A). They had markedly decreased hematocrit than WT embryos (Figure 1B). E14.5 p190-B$^{-/-}$ embryos were smaller in size (Figure 1A) and in weight (supplemental Figure S1A) than WT embryos. They had smaller fetal livers than WT littermates (Figure 1C) and the cellular content of p190-B$^{-/-}$ FL was 50% reduced compared to WT (Figure S1B). Because p190-B-deficiency is known to cause a cell size reduction, [20] the small fetal livers of p190-B$^{-/-}$ embryos could also reflect this cell size phenotype. However, the size of the cells contained in e14.5 FL was similar to that of WT FLs (Figure S1B,C), suggesting that additional mechanisms are responsible for the observed p190-B$^{-/-}$ fetal liver phenotype. Because FL is the major hematopoietic organ at midgestation where erythroid cells in particular undergo dramatic expansion, we further explored the fetal erythroid cell development. The numbers of late erythroid progenitors, CFU-erythroid, burst forming-unit (BFU) erythroid (E), colony forming-unit (CFU)-mix grown in the presence of EPO and SCF per p190-B$^{-/-}$ FL were significantly lower than WT (Figure 1D,E). Finally, examination of erythroid cell differentiation based on cell surface expression of CD71 and Ter119 [24], indicated reduction in late erythroid cells (CD71^{low}/Ter119^{high}) (Figure 1F and supplemental Table S2) in p190-B$^{-/-}$ animals. Overall, the total numbers of erythroid cells at each stage of differentiation were reduced in p190-B$^{-/-}$ embryos (supplemental Table S2).

During embryogenesis, the fetal bones are being colonized by fetal liver HSCs around e17. [4] Histological examination of bone section from femurs of WT e18.5 embryos showed the presence of erythroid and hematopoietic cell clusters. These hematopoietic clusters were absent from e18.5 p190-B$^{-/-}$ fetal bones (Figure 2A). Instead, the bones were filled with nonhematopoietic cells and extracellular matrix. Consistently, p190-B$^{-/-}$ fetal BM contained 50% and 16% reduction in CFU-GM and erythroid colonies, respectively, relative to WT littermates (Figure 2B). Immunophenotypic analysis of the CD45^{+} fraction of fetal bone

marrow showed lower frequencies of Long-Term-HSC ($Lin^{neg}Sca^{pos}Kit^{pos}CD150^{pos}CD48^{neg}$), Short-Term-HSC and multipotent progenitors (LSK), and progenitors (LK) in p190-$B^{-/-}$ embryos than WT littermates (Figure 2C). We previously demonstrated that p190-$B^{-/-}$ FL contained normal numbers of HSCs with greater self renewal ability than WT. P190-$B^{-/-}$ HSC/P did not have any intrinsic defect, in fact homing to the bone marrow or in SDF-1α-driven migration were increased [22]. Therefore, the hematopoietic defect seen in p190-$B^{-/-}$ embryos is likely an indication of impaired hematopoietic development in the bone marrow niche rather than a defect in bone colonization.

Hence, p190-B-deficiency led to multiple hematopoietic defects, including the myeloid and erythroid lineages, present at several stages of embryo development.

p190-$B^{+/-}$ mice exhibit non cell autonomous hematopoietic defects

To determine whether this phenotype was restricted to fetuses, we examined hematopoiesis of adult haploinsufficient animals, at least 6-weeks old. Most of these animals showed no alterations in hematopoietic parameters at steady state (not shown).

Interestingly, we noted that around 10% p190-$B^{+/-}$ animals (18 out of 150) developed significant abnormalities before 6-weeks of age, including brain hemorrhage and hematologic failure. Peripheral blood parameters indicated an abnormal relative proportion of myeloid cells and lymphoid cells, showing more granulocytes and less B lymphocytes. However, the proportion of T lymphocytes remained unchanged. (supplemental Table S3) Bone marrow analysis of p190-$B^{+/-}$ animals showed significantly lower LT-HSC and LSK frequencies than WT controls. This was associated with a decrease in B cells, whereas mature erythroblast cells were increased and granulocytes were unchanged. (Figure 3A) Finally, p190-$B^{+/-}$ mice had a marked decrease in spleen cellularity (Figure 3B), which was due to a decrease in all hematopoietic cells constituting the spleen – ie, B lymphoid, erythroid cells, as well as myeloid cells (not shown). Therefore, p190-B haploinsufficiency is associated with numerous hematopoietic abnormalities in a significant number of adult animals. However, none of the hematological defects associated with p190-B loss were transplantable. Mice reconstituted with p190-$B^{-/-}$ FL cells exhibited bone marrow content, white blood count, red blood count and hematocrit similar to those reconstituted with WT cells [22]. The numbers of myeloid CFUs, LT-HSC and LSK in the bone marrow of p190-$B^{-/-}$-reconstituted mice were comparable to WT. p190-$B^{-/-}$-reconstituted animals exhibited normal erythroid lineage differentiation at steady state (supplemental Figure S2A). Therefore, the hematopoietic abnormalities due to p190-B loss appear to be non-cell autonomous.

To further examine the cell extrinsic nature of p190-B-deficiency phenotype, we performed a ‘reverse transplantation’ assay in which WT bone marrow cells were transplanted into lethally irradiated WT and p190-$B^{+/-}$ recipients. Due to early death of the 10% p190-$B^{+/-}$ adult mice that exhibited hematopoietic abnormalities, this experiment was performed in randomly chosen ‘normal’ p190-$B^{+/-}$ animals. Four months following transplantation, p190-$B^{+/-}$ mice reconstituted with WT BoyJ cells exhibited a significant decrease in cellularity of both BM and spleen compared to WT controls (Figure S3A,B). p190-$B^{+/-}$ reconstituted

mice had a significant reduction in total numbers of LK and B220 cells in BM whereas the numbers of LSK and LT-HSC remained unchanged (Figure S3C,D). However, the blood parameters of these animals were normal (not shown). Although the phenotype of p190-B$^{+/-}$ reconstituted mice was modest, it supports the notion that the hematopoietic defects associated with p190-B-deficiency are non-cell autonomous.

p190-B$^{-/-}$ FL stromal cells do not support hematopoiesis

The hematopoietic microenvironment is composed of several cell types that support hematopoietic cells by providing physical support and secreting cytokines. [1-3] Mesenchymal progenitors are thought to be essential supportive cells in the embryo. In the fetal liver, there is a temporal correlation between the development of mesenchymal/stromal cells and hematopoietic progenitors. [25] To evaluate the function of p190-B$^{-/-}$ stromal/mesenchymal cells in hematopoietic supportive ability, MSCs from both genotypes were derived in culture. p190-B$^{-/-}$ FL, like WT, gave rise to primary stromal cell culture in vitro with morphological and phenotypical characteristics undistinguishable from WT. They exhibited a spindle/mesenchymal-like shape (Figure S4A). Stromal/mesenchymal progenitors derived from FL reportedly express CD90, Sca-1 and CD44. Most of the stromal cell lines derived from p190-B$^{-/-}$ FL cultures, like WT, co-expressed CD90, Sca-1 and CD44 but not CD105 or CD73, and they were negative for CD45, CD11b and CD31 expression, confirming a non-hematopoietic or endothelial cell origin (Figure S4B). We noticed some variability in the phenotype of these cells, and some did not express Sca-1 or CD90. To better compare their functions, all experiments hereafter were performed with primary culture of phenotypically matched stromal cells, ie CD90+CD44+Sca-1+, from early passages (p3-p7). The mRNA expressions of nestin, osteopontin, cdh2, which are known MSC markers, were not significantly different between WT and p190-B$^{-/-}$ stromal cells (Figure S4C).

Cobblestone area forming cells (CAFC) assay was then performed with stromal cells from both genotypes cocultured with various numbers of WT bone marrow cells (Figure 4A). CAFC are derived from HSC/P and have been proposed as surrogate assay to determine stroma-dependent hematopoiesis. In 5 independent experiments performed with 5 independent stroma, the frequency of CAFC, both at week 1 and week 2, was 75% reduced in culture initiated on p190-B$^{-/-}$stroma than those initiated on WT stroma (Figure 4A-C). CFU assay was also performed with hematopoietic cells recovered from one week coculture. Cocultures from p190-B$^{-/-}$stroma gave rise to 2-fold less CFU than WT stroma (Figure 4D), suggesting that p190-B$^{-/-}$ stromal cells are defective in supporting hematopoietic progenitors. A competitive repopulation assay using output cells from one week cocultures of WT BM cells and each stroma and fresh bone marrow competitor cells was used to assess HSC maintenance. Four months following transplantation, the frequency of CD45.2^{+} cells in the peripheral blood of mice that received cells cocultured on p190-B$^{-/-}$ stroma was dramatically reduced compared to mice that received cells cocultured on WT stroma, equivalent to a 100-fold difference in calculated competitive repopulation unit (Figure 4E). This is likely specific for p190-B expression loss in MSCs since p190-B knockdown in WT MSC abrogated their ability to support CFU-GM in coculture (Figure 4F,G). Therefore,

p190-B$^{-/-}$ FL mesenchymal/stroma cells are functionally defective in their ability to support hematopoiesis.

p190-B$^{-/-}$ FL and fetal BM microenvironment composition is altered

The hematopoietic microenvironment is composed of several cell types, including osteoblasts and adipocytes in the bone marrow. [1-3] An alteration in the cellular composition of the hematopoietic niche is likely to affect hematopoiesis. We thus seek to examine the cellular composition of the microenvironment in p190-B$^{-/-}$ embryos. In the fetal liver, the total number of non-hematopoietic cells, ie Ter119-CD45- cells, was dramatically reduced in p190-B$^{-/-}$ FL compared to WT (supplemental Figure S5 and S6A). Likewise, the content of immunophenotypically defined stromal populations CD105+CD73+ CD90+ and CD105+CD73+ CD90- was drastically reduced in p190-B$^{-/-}$ FL compared to WT (Figure S5 and S6A). This was also associated with less numbers of CFU-fibroblasts (CFU-F, hallmark marker of mesenchymal stem/progenitors) in p190-B$^{-/-}$ FL (Figure S6B). The BM content of various niche cell components was then assessed. p190-B$^{-/-}$ e18.5 fetal bones contained ~70% less CFU-F than their WT counterparts (Figure 5A). However, the presence of 'morphologically abnormal' CFU-F in p190-B$^{-/-}$ culture was noted (Figure 5A,B). In addition, the number of colonies composed of mature adipocytes was markedly lower in p190-B$^{-/-}$ fetal bones. Instead, p190-B$^{-/-}$ fetal BM culture gave rise to clusters of cells that were Oil-red-O positive in higher numbers than WT cultures (Figure 5A,B). Finally, osteogenic colony numbers (CFU-alkaline phosphatase positive, CFU-ALP) were 3-fold reduced in p190-B$^{-/-}$ fetal bones compared to WT, indicating impaired osteogenic differentiation (Figure 5A,B). Thus, the hematopoietic failure of p190-B$^{-/-}$ embryos is also associated with abnormal niche cellular composition.

p190-B$^{+/-}$ mice exhibit abnormal BM microenvironment

To examine the composition of the microenvironment of p190-B-haploinsufficient animals, bone histology was performed. Hematoxylin and eosin staining indicated an increase in adipocytes in p190-B$^{+/-}$ femur head sections compared to WT controls (Figure 5C). Interestingly, p190-B$^{+/-}$ femurs contained less osteoblasts and stromal-like cells that normally align along the endosteal region of the bones in WT (Figure 5D). To examine whether the apparent lack of osteoblasts was associated with less osteoblastic functions, we performed Masson's Trichrome staining for the detection of collagen fibers. Remarkably, p190-B$^{+/-}$ femur showed less collagen deposition, as seen by both less extend and lower intensity of staining, than their age-matched WT counterpart (Figure 5E and Figure S7). These data suggest that the bone marrow microenvironment of p190-B$^{+/-}$ mice is abnormal.

p190-B$^{-/-}$ MSCs have abnormal differentiation potential

Osteoblasts and adipocytes derive from a common MSC progenitor. [5] We next investigated whether the abnormal cellular composition of the microenvironment of p190-B-deficient animals was possibly due to abnormal MSC differentiation. We first examined their ability to give rise to CFU-F. Despite a decrease in the overall FL content of CFU-F (Figure S6B), the efficiency of generation of CFU-F of p190-B$^{-/-}$ FL stroma was ~2-fold higher than for WT FL stroma (Figure 6A). We next examined MSC differentiation to osteoblasts or adipocytes. WT cells gave rise to numerous ALP-positive osteoblastic cells

(Figure 6B). Correspondingly, expression of osteoblastic differentiation genes, including ALP, Runx2 and osteocalcin (Figure 6C) were upregulated relative to non-induced cultured cells. In contrast, the generation of ALP-positive cells in p190-B$^{-/-}$ differentiated cultures was dramatically reduced, and the upregulation of ALP and Runx2 expression remained significantly lower than WT (Figure 6B,C), thus confirming impaired osteoblastic differentiation in p190-B$^{-/-}$ cells. Finally, in adipocytic differentiation cultures, p190-B$^{-/-}$cultures showed more Oil-red O-positive cells than WT cultures. This was associated with higher upregulation of the adipocytic transcription factors Pparγ and Cebp/α (Figure 6D,E). Thus, p190-B$^{-/-}$ cultured-derived mesenchymal progenitors have increased adipocytic and decreased osteogenic differentiation potential. Hence, the abnormal composition of the p190-B$^{-/-}$ fetal bone microenvironment may arise from impaired MSC differentiation along the osteoblastic and adipocytic lineages – a phenotype that may contribute to defective hematopoiesis.

Impaired hematopoietic support of p190-B$^{-/-}$ FL stroma is secondary to deficient expression of Wnt3a

Finally, to analyze the underlying molecular mechanism of p190-B in hematopoietic supportive activity, we examined the expression of various genes important for early hematopoietic and erythroid development and for HSC maintenance in the niche, using quantitative RT-PCR. The expressions of erythropoietin and thrombopoietin in p190-B$^{-/-}$ FL or in FL-derived stromal cells were similar to that of WT cells (Figure S8). However, the expression of angiopoietin, Bmp4, Cxcl12, also known to support HSC functions and stemness, were higher in p190-B$^{-/-}$ stromal cells relative to WT cells (Figure 7A). Expression of c-kit ligand was unchanged (Figure S8) Conversely, mRNA expression of Wnt3a was markedly lower (Figure 7A). Some p190-B$^{-/-}$ stromal cells also exhibited less expression of Tcf/Lef1, a key target of Wnt signaling. This apparent abnormal Wnt signaling was associated with the upregulation of negative regulators of Wnt signaling, including secreted frizzled-related proteins (Sfrp1 and Sfrp2) (Figure 7A). Of interesting note, and consistent with abnormal adipocytic differentiation in p190-B$^{-/-}$ embryos, leptin expression, which is known to be secreted by adipocytes, was significantly lower in p190-B$^{-/-}$ calvaria bones than in WT (Figure S8).

Because Wnt3a can contribute to hematopoietic supportive activity of stromal cells [26], we tested whether the lack of Wnt3a mRNA expression in p190-B$^{-/-}$ stroma could account for their impaired functions. First, the lack of Wnt3a expression was specific for p190-B loss since its expression became undetectable in p190-B knock down stroma (Figure 7B). We then performed coculture experiments supplemented with recombinant Wnt3a (rWnt3a). Remarkably, rWnt3a restored the ability of p190-B$^{-/-}$ stroma to maintain hematopoietic progenitor activity, as assessed by CFU assay (Figure 7C) and CAFC frequency (Figure 7D). Thus, Wnt3a may contribute to p190-B extrinsic regulation of hematopoiesis.

Altogether, these data suggest that p190-B is critical for hematopoiesis in a non-cell autonomous manner. This is possibly due to synergistic effects of two mechanisms: one that controls the expression of cytokines that are important for HSC and progenitor functions by

MSCs, a second that regulates the cellular composition of the hematopoietic niche by MSC differentiation.

Discussion

The study presented here provides evidence that p190-B RhoGAP is a critical regulator of hematopoiesis in a non-cell autonomous manner. p190-B appears to control hematopoietic supportive activity of mesenchymal stem/progenitor cells in vitro. Concomitantly, p190-B is necessary for a proper cellular composition of the hematopoietic niche that may be due to abnormal mesenchymal-derived lineage specification. Therefore, our study suggests that p190-B is essential to shape a functional hematopoietic niche during development.

Homozygous mutant p190-B mice die immediately after birth because their lungs fail to inflate properly, and they always exhibit a substantial reduction in size [20]. Here, we show that p190-B-deficiency causes a number of hematopoietic defects both in embryos and adults, and affecting HSCs, and myeloid, B cell and erythroid lineages. None of these hematopoietic anomalies are transplantable into adult WT recipients. In fact, p190-B loss improves HSC self renewal during serial transplantation without altering their multipotent hematopoietic lineage differentiation [22]. Conversely, p190-B heterozygotes mice reconstituted with WT BM cells exhibited a modest decrease in BM and spleen cellularity and a decrease in B lineages. Therefore, the abnormal hematopoiesis seen in p190-B-deficient animals is likely non-cell autonomous. The hematopoietic defects seen in fetal bones could result from a decrease in the pool of HSC that developed in the fetal liver and/or an abnormal hematopoietic colonization of the fetal bones. This seems unlikely, since 1) the number of HSCs is normal in p190-B-deficient FLs, [22] 2) the migratory capacity to CXCL12, which is responsible for HSC bone colonization,[27] of p190-B-deficient HSC/Ps, as well as their homing to WT bone marrow, were higher than those of WT cells, [22] 3) p190-B-deficient stromal cells express CXCL12. Therefore, p190-B emerges as an essential extrinsic regulator of hematopoiesis.

Differences were observed in the phenotype of p190-B$^{-/-}$ embryos and ten percent of p190-B haploinsufficient animals that do not survive, notably in the erythroid lineage. Mature erythroblasts were decreased in p190-B$^{-/-}$ embryos but increased in these p190-B heterozygotes animals. Because p190-B$^{-/-}$ erythroid progenitors differentiated normally in vitro (unpublished data, M-D.F), the difference is likely not cell-intrinsic. The differences may come from distinct regulation of erythropoiesis by different microenvironment during ontogeny – ie, FL versus adult BM. The best-known niche for erythropoiesis is the erythroblastic island, which is composed of a central macrophage that provides survival and proliferative factors to the surrounding erythroblasts. [28] This blood island is critical for fetal liver and adult bone marrow erythropoiesis. However, the bone marrow microenvironment offers many other regulatory cells than the FL that may impart erythropoiesis, although largely unknown. [29] For instance, erythropoiesis appears to be linked to bone homeostasis via osteoblast/osteoclast function. The increase in erythroid cells in p190-B+/- adults may also be a secondary response to hormones secreted by other organs, such as the parathyroid gland. [29]

At a mechanistic level, our study suggests that p190-B controls hematopoiesis by two potential and synergistic non-cell autonomous mechanisms resulting from dysfunctional mesenchymal stem/progenitor cells. p190-B regulates the cellular composition of the microenvironment, as well as the secretion of regulatory factors by MSCs. The niche is composed of several cell types. An optimal proportion of various niche constituents, in particular a balance in osteoblasts and adipocytes, must be maintained for normal hematopoiesis. Osteoblasts are important HSC regulatory cells by producing hematopoietic cytokines. Increasing the numbers of osteoblasts in BM concomitantly increases HSC numbers. [16, 30] Conversely, ablation of osteoblasts leads to a marked decrease HSCs and hematopoietic progenitors. [31] On the other hand, adipocytes are thought to negatively impact hematopoiesis. [17] p190-B$^{-/-}$ embryos have fewer CFU-F, less osteolineage development than WT. p190-B loss also causes an abnormal adipocyte development. The unbalance osteoblastic/adipocytic lineages may arise from a failure to establish a proper niche during development. Indeed, these lineages derive from a common MSC progenitor [5, 32]. MSCs contribute to early bone, bone marrow, skeleton, [7] and also cartilage and spleen development. Using ectopic bone formation, CD146^{+} MSCs isolated from human bone marrow or CD105^{+} cells from mouse fetal bones can establish a niche for HSC [8, 9]. Nestin^{+} bone marrow MSCs can give rise to osteoblasts, adipocytes and chondrocytes in in vivo lineage tracing experiments, and in ectopic bone assay [10]. p190-B-deficient MSCs have an abnormal differentiation along the osteoblastic and adipocytic lineages. Hence, the defective hematopoiesis in p190-B-deficient animals likely results from a failure in establishing and maintaining the proper cellular composition of the hematopoietic niche.

Another possible level of regulation is through the secretion of factors that are critical for hematopoietic cell homeostasis by mesenchymal/stromal cells. MSCs are thought to also act as regulatory cells by secreting soluble factors, including CXCL12, c-KIT ligand, angiopoietin. [10] In the embryo, they encompass for the majority of the hematopoietic supportive activity of the microenvironment. [7, 33, 34] p190-B$^{-/-}$ MSCs fail to support hematopoietic activity in ex vivo coculture. Our gene expression analysis reveals that many regulatory molecules known to control hematopoiesis are in fact normally expressed or upregulated in p190-B$^{-/-}$ stromal cells, including Ang, c-KitL, CXCL12, BMP4, osteopontin [16, 35-42]. However, Wnt3a was downregulated and supplementing p190-B$^{-/-}$ stroma with rWnt3a could restore their ability to support WT hematopoietic progenitors in coculture. The role of Wnt signaling in hematopoiesis is complex, and context- and dosage-dependent. Nevertheless, Wnt3a was necessary for normal hematopoiesis and long term HSC functions in the fetal liver [43, 44]. Addition of Wnt3a maintains HSC ‘stemness’ in coculture with stromal cells [26]. In vivo, increased Wnt signaling enhances HSC repopulation capacity [45], whereas inhibition of Wnt signaling, by expression of Dkk transgene or the Wnt-pan inhibitor Wif in osteoblasts, yielded HSC defects [46, 47]. Other interesting genes are sfrp1 and sfrp2 whose expressions were upregulated in p190-B-deficient stroma. Both Sfrp1 and Sfrp2 are negative modulators of canonical and non-canonical Wnt signaling [48] and can modulate HSC maintenance [49]. The defect in Wnt3a expression by MSCs could also contribute to the defective erythropoiesis, at least in the FL. Indeed, Wnt signaling appears to be important for erythroid lineage differentiation. [50] The lack of Wnt3a may also contribute to the unbalance osteoblast and adipocytic lineages in

p190-B-deficient embryos since Wnt signaling can control the MSC differentiation along these lineages. [51] The relationship between p190-B and Wnt3a expression has not been established before. Surprisingly, despite the importance of Wnt ligands for embryo development, little is known about their transcriptional regulation. In our model, the involvement of RhoA activity is likely. p190-B is a potent RhoA inhibitor and most of the functions controlled by p190-B have been attributed to its effect on RhoA activity. [20-21] For instance, RhoA controls gene expression via activation of the transcription factor SRF (serum responsive factor). [52] p190-B can regulate the activity of the transcription factor Creb in fibroblasts. [20-21] Since SRF and Creb have both been implicated in stromal/mesenchymal cell functions, [53-54] their participation in p190-B regulation of Wnt3a mRNA expression is possible. Interestingly, there is evidence that the RhoA effector focal adhesion kinase (FAK) can translocate to the nucleus and regulate Wnt3a mRNA expression in neural and cancer cells. [55]

Another interesting observation is the decrease in leptin mRNA expression in p190-B-deficient bones, which likely arises from their abnormal adipocyte differentiation. Indeed, leptin, the product of the *obese* gene, is primarily secreted by adipocytes. [56] It regulates nutrient intake and metabolism. Interestingly, leptin can stimulate hematopoietic lineages, including erythroid cells. [57-59] Leptin-deficient mice had only 60% of nucleated cells in their BM compared to control, with further decrease of the B cell compartment (70%). [57] Leptin has also been shown to increase the sensitivity of erythroid cells to erythropoietin in patients. [60] Intriguingly, leptin plays a critical but dual role in bone homeostasis [61,62]; notably, it can directly increase osteoblast proliferation and differentiation, and decrease adipogenesis. [63] This raises the possibility that the reduction in leptin in p190-B-deficient embryos may contribute to their abnormal hematopoiesis. Hence, it is likely that other factor than Wnt3a, including leptin and cell-cell interaction, mediate p190-B effect on the hematopoietic microenvironment. These factors may differentially regulate HSC, and the myeloid and erythroid progenitors. It will be interesting to dissect in detail these mechanisms. Together, these observations suggest that the hematopoietic defects seen in absence of p190-B arise from multiple and potentially synergistic effects of dysfunctional MSCs, both as regulatory cells and as niche-forming cells.

The role of p190-B in hematopoiesis appears multiple. We previously reported that p190-B negatively controls HSC self-renewal. During serial competitive repopulation assay, p190-B-deficiency confers to HSCs better self-renewal ability than their WT counterpart. [22] Hence, p190-B seems to have opposite role on hematopoiesis: a positive role by maintaining a proper hematopoietic niche but a negative role on intrinsic HSC functions. It is unclear how p190-B functions. Regulation of RhoA signaling likely contributes to its function. For example, RhoA has been shown to control MSC differentiation into osteoblasts and adipocytes. [15] But, p190-B is a multiple domain protein that may also function independently of RhoA signaling [64]. P190-B functions may depend on the cellular context. In addition, cell-cell communication between the niche constituents likely further influences the outcome of p190-B deregulation in MSCs. Of interesting note, current studies in our laboratory suggest that p190-B regulates HSC self-renewal by controlling HSC fate decision to self-renew or to differentiate during division (manuscript in preparation, A.H. &

M-D.F). P190-B also regulates a MSC decision to differentiate to adipocytes or myocytes. [21] Studies presented here suggest that p190-B controls MSC fate differentiation to adipocyte and osteoblasts. It is tempting to speculate that p190-B acts a master regulator of stem cell fate decisions, the outcome of which will depend on the cellular and environmental context.

In the past decade, Rho GTPases have been established as key regulators of hematopoietic cell functions. [13] Surprisingly, little is known about their contribution to the hematopoietic niche. In this regards, it will be important to investigate the contribution of RhoA signaling to p190-B phenotype. Rac1 deletion in osteoblasts was associated with reduction in bone mass, although this phenotype had no impact on hematopoiesis. [65] Cdc42 is important for bone remodeling and skeletal mineralization. [66,67] But the consequences on hematopoiesis are unknown. Rho GTPases are pleiotropic regulators of cellular homeostasis. Their role in the hematopoietic microenvironment is likely but still need to be further investigated in specific context.

In conclusion, our study identified a novel regulatory pathway of MSC functions that is critical for maintaining normal hematopoiesis in vivo. There remain fundamental issues on the existence of true MSCs in vivo and their participation in niche formation. Our study raises intriguing questions on the exact identity of p190-B-deficient MSCs and whether the broad defects in mesenchymal-lineages solely results from the dysfunction of a nonhematopoietic stem cell. The development of a conditional p190-B deletion model, which is currently not available, and lineage tracing experiments will be essential to address this important issue. MSCs and hematopoietic microenvironment dysfunctions are associated with bone marrow failure or cancer. [11,12,68,69] MSCs hold great promises for regenerative medicine given their potent ability for tissue repair in vivo. Hence, our findings are highly important for our understanding of the formation of the HSC niche; and have broad implication for hematopoietic disorders and regenerative medicine.

Supplementary Material

Refer to Web version on PubMed Central for supplementary material.

ACKNOWLEDGEMENTS

We thank the mouse core, Jeff Bailey and Victoria Summey, for bone marrow transplantation and the Flow Cytometry core for assistance with cell sorting at Cincinnati Children's Hospital Medical Center.

The work was supported by NIH (HL090676 and HL104458-MDF).

Literature Cited

1. Shiozawa Y, Havens AM, Pienta KJ, Taichman RS. The bone marrow niche: habitat to hematopoietic and mesenchymal stem cells, and unwitting host to molecular parasites. Leukemia. 2008; 22:941–590. [PubMed: 18305549]
2. Yin T, Li L. The stem cell niches in bone. J Clin Invest. 2006; 116(5):1195–201. [PubMed: 16670760]
3. Kiel MJ, Morrison SJ. Uncertainty in the niches that maintain haematopoietic stem cells. Nat Rev Immunol. 2008; 8(4):290–301. [PubMed: 18323850]

4. Mikkola HK, Orkin SH. The journey of developing hematopoietic stem cells. Development. 2006; 133(19):3733–44. [PubMed: 16968814]
5. Caplan AI. Mesenchymal stem cells. J Orthop Res. 1991; 9(5):641–50. [PubMed: 1870029]
6. Friedenstein AJ, Chailakhyan RK, Latsinik NV, Panasyuk AF, Keiliss-Borok IV. Stromal cells responsible for transferring the microenvironment of the hemopoietic tissues. Cloning in vitro and retransplantation in vivo. Transplantation. 1974; 17(4):331–40. [PubMed: 4150881]
7. Arai F, Ohneda O, Miyamoto T, Zhang XQ, Suda T. Mesenchymal stem cells in perichondrium express activated leukocyte cell adhesion molecule and participate in bone marrow formation. J Exp Med. 2002; 195(12):1549–63. [PubMed: 12070283]
8. Sacchetti B, Funari A, Michienzi S, Di Cesare S, Piersanti S, Saggio I, et al. Self-renewing osteoprogenitors in bone marrow sinusoids can organize a hematopoietic microenvironment. Cell. 2007; 131(2):324–36. [PubMed: 17956733]
9. Chan CK, Chen CC, Luppen CA, Kim JB, DeBoer AT, Wei K, et al. Endochondral ossification is required for haematopoietic stem-cell niche formation. Nature. 2009; 457(7228):490–4. [PubMed: 19078959]
10. Mendez-Ferrer S, Michurina TV, Ferraro F, Mazloom AR, Macarthur BD, Lira SA, et al. Mesenchymal and haematopoietic stem cells form a unique bone marrow niche. Nature. 2010; 466(7308):829–34. [PubMed: 20703299]
11. Lecourt S, Vanneaux V, Leblanc T, Leroux G, Ternaux B, Benbunan M, et al. Bone marrow microenvironment in fanconi anemia: a prospective functional study in a cohort of fanconi anemia patients. Stem Cells Dev. 2010; 19(2):203–8. [PubMed: 19572808]
12. Dror Y, Freedman MH. Shwachman-Diamond syndrome: An inherited preleukemic bone marrow failure disorder with aberrant hematopoietic progenitors and faulty marrow microenvironment. Blood. 1999; 94(9):3048–54. [PubMed: 10556188]
13. Mulloy JC, Cancelas JA, Filippi M-D, Kalfa T, Guo F, Zheng Y. Rho GTPases in hematopoiesis and hemopathies. Blood. 2010; 115(5):936–47. [PubMed: 19965643]
14. Hall A. G Proteins and Small GTPases: Distant Relatives Keep in Touch. Science. 1998; 280:2074–2075. [PubMed: 9669963]
15. McBeath R, Pirone DM, Nelson CM, Bhadriraju K, Chen CS. Cell shape, cytoskeletal tension, and RhoA regulate stem cell lineage commitment. Dev Cell. 2004; 6(4):483–95. [PubMed: 15068789]
16. Calvi LM, Adams GB, Weibrecht KW, Weber JM, Olson DP, Knight MC, et al. Osteoblastic cells regulate the haematopoietic stem cell niche. Nature. 2003; 425(6960):841–6. [PubMed: 14574413]
17. Naveiras O, Nardi V, Wenzel PL, Hauschka PV, Fahey F, Daley GQ. Bone-marrow adipocytes as negative regulators of the haematopoietic microenvironment. Nature. 2009; 460(7252):259–63. [PubMed: 19516257]
18. Burbelo PD, Miyamoto S, Utani A, Brill S, Yamada KM, Hall A, et al. p190-B, a new member of the Rho GAP family, and Rho are induced to cluster after integrin cross-linking. J Biol Chem. 1995; 270(52):30919–26. [PubMed: 8537347]
19. Chakravarty G, Hadsell D, Buitrago W, Settleman J, Rosen JM. p190-B RhoGAP regulates mammary ductal morphogenesis. Mol Endocrinol. 2003; 17(6):1054–65. [PubMed: 12637587]
20. Sordella R, Classon M, Hu KQ, Matheson SF, Brouns MR, Fine B, et al. Modulation of CREB activity by the Rho GTPase regulates cell and organism size during mouse embryonic development. Dev Cell. 2002; 2(5):553–65. [PubMed: 12015964]
21. Sordella R, Jiang W, Chen GC, Curto M, Settleman J. Modulation of Rho GTPase signaling regulates a switch between adipogenesis and myogenesis. Cell. 2003; 113(2):147–58. [PubMed: 12705864]
22. Xu H, Eleswarapu S, Geiger H, Szczur K, Daria D, Zheng Y, et al. Loss of the Rho GTPase activating protein p190-B enhances hematopoietic stem cell engraftment potential. Blood. 2009
23. Geiger H, True JM, Grimes B, Carroll EJ, Fleischman RA, Van Zant G. Analysis of the hematopoietic potential of muscle-derived cells in mice. Blood. 2002; 100(2):721–3. [PubMed: 12091375]
24. Zhang J, Socolovsky M, Gross AW, Lodish HF. Role of Ras signaling in erythroid differentiation of mouse fetal liver cells: functional analysis by a flow cytometry-based novel culture system. Blood. 2003; 102(12):3938–46. [PubMed: 12907435]

25. Wolf NS, Bertoncello I, Jiang D, Priestley G. Developmental hematopoiesis from prenatal to young-adult life in the mouse model. Exp Hematol. 1995; 23(2):142–6. [PubMed: 7828671]
26. Kim JA, Kang YJ, Park G, Kim M, Park YO, Kim H, et al. Identification of a stroma-mediated Wnt/beta-catenin signal promoting self-renewal of hematopoietic stem cells in the stem cell niche. Stem Cells. 2009; 27(6):1318–29. [PubMed: 19489023]
27. Ratajczak MZ, Zuba-Surma E, Kucia M, Reca R, Wojakowski W, Ratajczak J. The pleiotropic effects of the SDF-1–CXCR4 axis in organogenesis, regeneration and tumorigenesis. Leukemia. 2006; 20:1915–1924. [PubMed: 16900209]
28. Chasis JA, Mohandas N. Erythroblastic islands: niches for erythropoiesis. Blood. 2008; 112(3): 470–8. [PubMed: 18650462]
29. Walkley CR. Erythropoiesis, anemia and the bone marrow microenvironment. Int J Hematol. 2011; 93(1):10–3. [PubMed: 21222184]
30. Zhang J, Niu C, Ye L, Huang H, He X, Tong WG, et al. Identification of the haematopoietic stem cell niche and control of the niche size. Nature. 2003; 425(6960):836–41. [PubMed: 14574412]
31. Visnjic D, Kalajzic Z, Rowe DW, Katavic V, Lorenzo J, Aguila HL. Hematopoiesis is severely altered in mice with an induced osteoblast deficiency. Blood. 2004; 103(9):3258–64. [PubMed: 14726388]
32. Pittenger MF, Mackay AM, Beck SC, Jaiswal RK, Douglas R, Mosca JD, et al. Multilineage potential of adult human mesenchymal stem cells. Science. 1999; 284(5411):143–7. [PubMed: 10102814]
33. Badillo AT, Flake AW. The regulatory role of stromal microenvironments in fetal hematopoietic ontogeny. Stem Cell Rev. 2006; 2(3):241–6. [PubMed: 17625260]
34. Bianco P. Bone and the hematopoietic niche: a tale of two stem cells. Blood. 2011; 117(20):5281–8. [PubMed: 21406722]
35. Arai F, Hirao A, Ohmura M, Sato H, Matsuoka S, Takubo K, et al. Tie2/angiopoietin-1 signaling regulates hematopoietic stem cell quiescence in the bone marrow niche. Cell. 2004; 118(2):149–61. [PubMed: 15260986]
36. Nilsson SK, ohnston HM, Whitty GA, Williams B, Webb RJ, Denhardt DT, et al. Osteopontin, a key component of the hematopoietic stem cell niche and regulator of primitive hematopoietic progenitor cells. Blood. 2005; 106(4):1232–9. [PubMed: 15845900]
37. Stier S, Ko Y, Forkert R, Lutz C, Neuhaus T, Grünewald E, et al. Osteopontin is a hematopoietic stem cell niche component that negatively regulates stem cell pool size. J Exp Med. 2005; 201(11):1781–91. [PubMed: 15928197]
38. Ding L, Saunders TL, Enikolopov G, Morrison SJ. Endothelial and perivascular cells maintain haematopoietic stem cells. Nature. 2012; 481(7382):457–62. [PubMed: 22281595]
39. Yoshihara H, Arai F, Hosokawa K, Hagiwara T, Takubo K, Nakamura Y, et al. Thrombopoietin/MPL signaling regulates hematopoietic stem cell quiescence and interaction with the osteoblastic niche. Cell Stem Cell. 2007; 1(6):685–97. [PubMed: 18371409]
40. Kollet O, Dar A, Shivtiel S, Kalinkovich A, Lapid K, Sztainberg Y, et al. Osteoclasts degrade endosteal components and promote mobilization of hematopoietic progenitor cells. Nat Med. 2006; 12(6):657–64. [PubMed: 16715089]
41. Peled A, Petit I, Kollet O, Magid M, Ponomaryov T, Byk T, et al. Dependence of human stem cell engraftment and repopulation of NOD/SCID mice on CXCR4. Science. 1999; 283(5403):845–8. [PubMed: 9933168]
42. Nagasawa T, Hirota S, Tachibana K, Takakura N, Nishikawa S, Kitamura Y, et al. Defects of B-cell lymphopoiesis and bone-marrow myelopoiesis in mice lacking the CXC chemokine PBSF/SDF-1. Nature. 1996; 382(6592):635–8. [PubMed: 8757135]
43. Luis TC, Naber BA, Fibbe WE, van Dongen JJ, Staal FJ. Wnt3a nonredundantly controls hematopoietic stem cell function and its deficiency results in complete absence of canonical Wnt signaling. Blood. 2010; 116(3):496–7. [PubMed: 20651084]
44. Luis TC, Weerkamp F, Naber BA, Baert MR, de Haas EF, Nikolic T, et al. Wnt3a deficiency irreversibly impairs hematopoietic stem cell self-renewal and leads to defects in progenitor cell differentiation. Blood. 2009; 113(3):546–54. [PubMed: 18832654]

45. Luis TC, Naber BA, Roozen PP, Brugman MH, de Haas EF, Ghazvini M, et al. Canonical wnt signaling regulates hematopoiesis in a dosage-dependent fashion. Cell Stem Cell. 2011; 9(4):345–56. [PubMed: 21982234]
46. Fleming HE, Janzen V, Lo Celso C, Guo J, Leahy KM, Kronenberg HM, Scadden DT. Wnt signaling in the niche enforces hematopoietic stem cell quiescence and is necessary to preserve self-renewal in vivo. Cell Stem Cell. 2008; 2(3):274–83. [PubMed: 18371452]
47. Schaniel C, Sirabella D, Qiu J, Niu X, Lemischka IR, Moore KA. Wnt-inhibitory factor 1 dysregulation of the bone marrow niche exhausts hematopoietic stem cells. Blood. 2011; 118(9): 2420–9. [PubMed: 21652676]
48. Kawano Y, Kypta R. Secreted antagonists of the Wnt signalling pathway. J Cell Sci. 2003; 116(Pt 13):2627–34. [PubMed: 12775774]
49. Renstrom J, Istvanffy R, Gauthier K, Shimono A, Mages J, Jardon-Alvarez A, et al. Secreted frizzled-related protein 1 extrinsically regulates cycling activity and maintenance of hematopoietic stem cells. Cell Stem Cell. 2009; 5(2):157–67. [PubMed: 19664990]
50. Trompouki E, Bowman TV, Lawton LN, Fan ZP, Wu DC, DiBiase A, et al. Lineage regulators direct BMP and Wnt pathways to cell-specific programs during differentiation and regeneration. Cell. 2011; 147(3):577–89. [PubMed: 22036566]
51. Ross SE, Hemati N, Longo KA, Bennett CN, Lucas PC, Erickson RL, MacDougald OA. Inhibition of adipogenesis by Wnt signaling. Science. 2000; 289(5481):950–3. [PubMed: 10937998]
52. Hill CS, Wynne J, Treisman R. The Rho family GTPases RhoA, Rac1, and CDC42Hs regulate transcriptional activation by SRF. Cell. 1995; 81(7):1159–70. [PubMed: 7600583]
53. Beqaj S, Jakkaraju S, Mattingly RR, Pan D, Schuger L. High RhoA activity maintains the undifferentiated mesenchymal cell phenotype, whereas RhoA down-regulation by laminin-2 induces smooth muscle myogenesis. J Cell Biol. 2002; 156(5):893–903. [PubMed: 11877460]
54. Kim JM, Choi JS, Kim YH, Jin SH, Lim S, Jang HJ, Kim KT, Ryu SH, Suh PG. An activator of the cAMP/PKA/CREB pathway promotes osteogenesis from human mesenchymal stem cells. J Cell Physiol. 2013; 228(3):617–26. [PubMed: 22886506]
55. Fonar Y, Gutkovich YE, Root H, Malyarova A, Aamar E, Golubovskaya VM, Elias S, Elkouby YM, Frank D. Focal adhesion kinase protein regulates Wnt3a gene expression to control cell fate specification in the developing neural plate. Mol Biol Cell. 2011; 22(13):2409–21. [PubMed: 21551070]
56. Zhang Y, Proenca R, Maffei M, Barone M, Leopold L, Friedman JM. Positional cloning of the mouse obese gene and its human homologue. Nature. 1994; 372(6505):425–32. [PubMed: 7984236]
57. Claycombe K, King LE, Fraker PJ. A role for leptin in sustaining lymphopoiesis and myelopoiesis. Proc Natl Acad Sci U S A. 2008; 105(6):2017–21. [PubMed: 18250302]
58. Umemoto Y, Tsuji K, Yang FC, Ebihara Y, Kaneko A, Furukawa S, et al. Leptin stimulates the proliferation of murine myelocytic and primitive hematopoietic progenitor cells. Blood. 1997; 90(9):3438–43. [PubMed: 9345027]
59. Bennett BD, Solar GP, Yuan JQ, Mathias J, Thomas GR, Matthews W. A role for leptin and its cognate receptor in hematopoiesis. Curr Biol. 1996; 6(9):1170–80. [PubMed: 8805376]
60. Axelsson J, Qureshi AR, Heimbürger O, Lindholm B, Stenvinkel P, Bárány P. Body fat mass and serum leptin levels influence epoetin sensitivity in patients with ESRD. Am J Kidney Dis. 2005; 46(4):628–34. [PubMed: 16183417]
61. Ducy P, Amling M, Takeda S, Priemel M, Schilling AF, Beil FT, et al. Leptin inhibits bone formation through a hypothalamic relay: a central control of bone mass. Cell. 2000; 100(2):197–207. [PubMed: 10660043]
62. Elefteriou F, Ahn JD, Takeda S, Starbuck M, Yang X, Liu X, et al. Leptin regulation of bone resorption by the sympathetic nervous system and CART. Nature. 2005; 434(7032):514–20. [PubMed: 15724149]
63. Scheller EL, Song J, Dishowitz MI, Soki FN, Hankenson KD, Krebsbach PH. Leptin functions peripherally to regulate differentiation of mesenchymal progenitor cells. Stem Cells. 2010; 28(6): 1071–80. [PubMed: 20506495]

64. Matheson SF, Hu KQ, Brouns MR, Sordella R, VanderHeide JD, Settleman J. Distinct but overlapping functions for the closely related p190 RhoGAPs in neural development. Dev Neurosci. 2006; 28(6):538–50. [PubMed: 17028431]

65. Lane SW, De Vita S, Alexander KA, Karaman R, Milsom MD, Dorrance AM, et al. Rac signaling in osteoblastic cells is required for normal bone development but is dispensable for hematopoietic development. Blood. 2012; 119(3):736–44. [PubMed: 22123845]

66. Zou W, Greenblatt MB, Shim JH, Kant S, Zhai B, Lotinun S, et al. MLK3 regulates bone development downstream of the faciogenital dysplasia protein FGD1 in mice. J Clin Invest. 2011; 121(11):4383–92. [PubMed: 21965325]

67. Ito Y, Teitelbaum SL, Zou W, Zheng Y, Johnson JF, Chappel J, et al. Cdc42 regulates bone modeling and remodeling in mice by modulating RANKL/M-CSF signaling and osteoclast polarization. J Clin Invest. 2010; 120(6):1981–93. [PubMed: 20501942]

68. Zhu Y, Sun Z, Han Q, Liao L, Wang J, Bian C, Li J, Yan X, Shao C, Zhao RC. Human mesenchymal stem cells inhibit cancer cell proliferation by secreting DKK-1. Leukemia. 2009; 23:925–933. [PubMed: 19148141]

69. Ayala F, Dewar R, Kieran M, Kalluri R. Contribution of bone marrow microenvironment to leukemogenesis and leukemia progression. Leukemia. 2009; 23:2233–2241. [PubMed: 19727127]

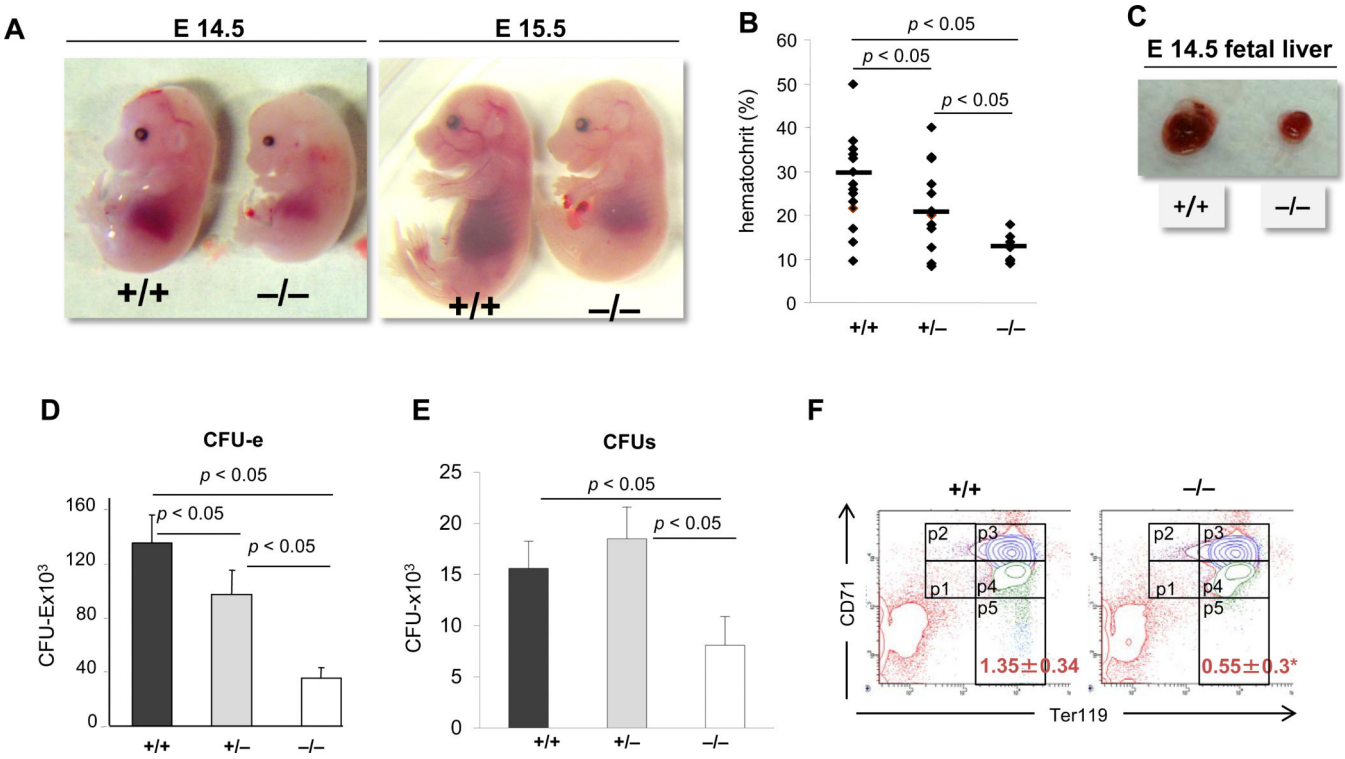

Figure 1. Fetal liver hematopoietic defects in p190-B$^{-/-}$ embryos

(A) Images of embryonic day14.5 and day 15.5. **(B)** Hematocrit of peripheral blood of e14.5 embryos. **(C)** Pictures of fetal liver of e14.5 embryos. **(D&E)** Fetal liver cells were plated in methylcellulose with EPO and SCF. Colonies were scored at day 2 for CFU-e (D) and day 7 for CFU-mix (E). Histogram is total number of colonies per liver (mean±SD, n=8). **(F)** Representative flow cytometry chart of fetal liver erythroid differentiation profile assessed by Ter119 and CD71 expression profile, P1: Ter119^{low}CD71^{low}; P2: Ter119^{low}CD71^{high}; P3: Ter119^{high}CD71^{high}; P4: Ter119^{high}CD71^{Int}; P5: Ter119^{high}CD71^{low} see supplemental table 1 for quantifications.

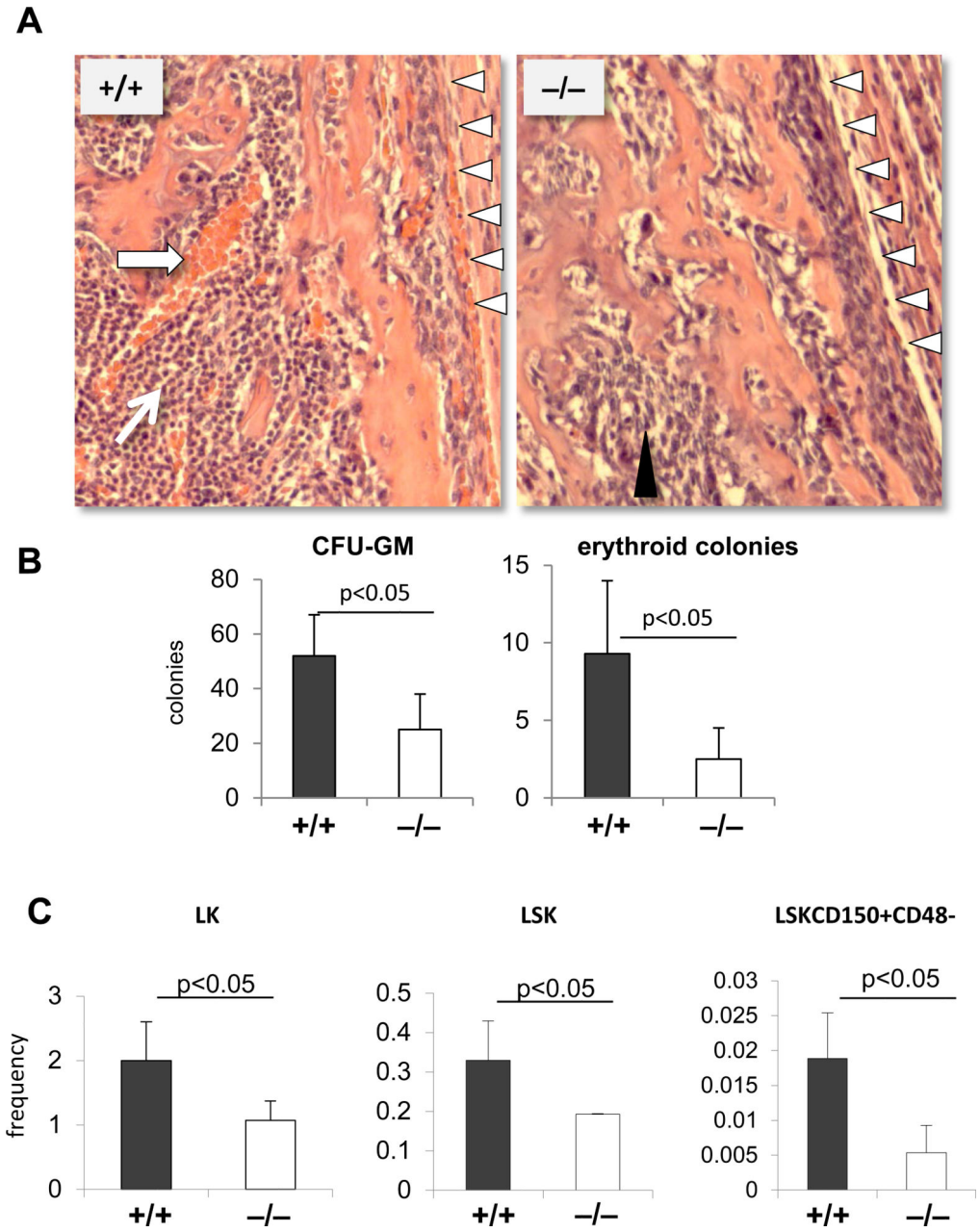

Figure 2. Bone marrow hematopoietic defects in p190-B$^{-/-}$ embryos

(A) H&E staining of fetal bone section at e18.5. Arrows point to hematopoietic clusters, black arrow heads point to non-hematopoietic cells, white arrow heads points to endosteal bone region (n=4). **(B)** Total number of CFU-GM and BFU-E colonies per e18.5 bone (mean±SD, n=4). **(C)** Frequency of LT-HSC, LSK and LK within CD45+ fraction of e18.5 bone marrow (mean±SD, n=5).

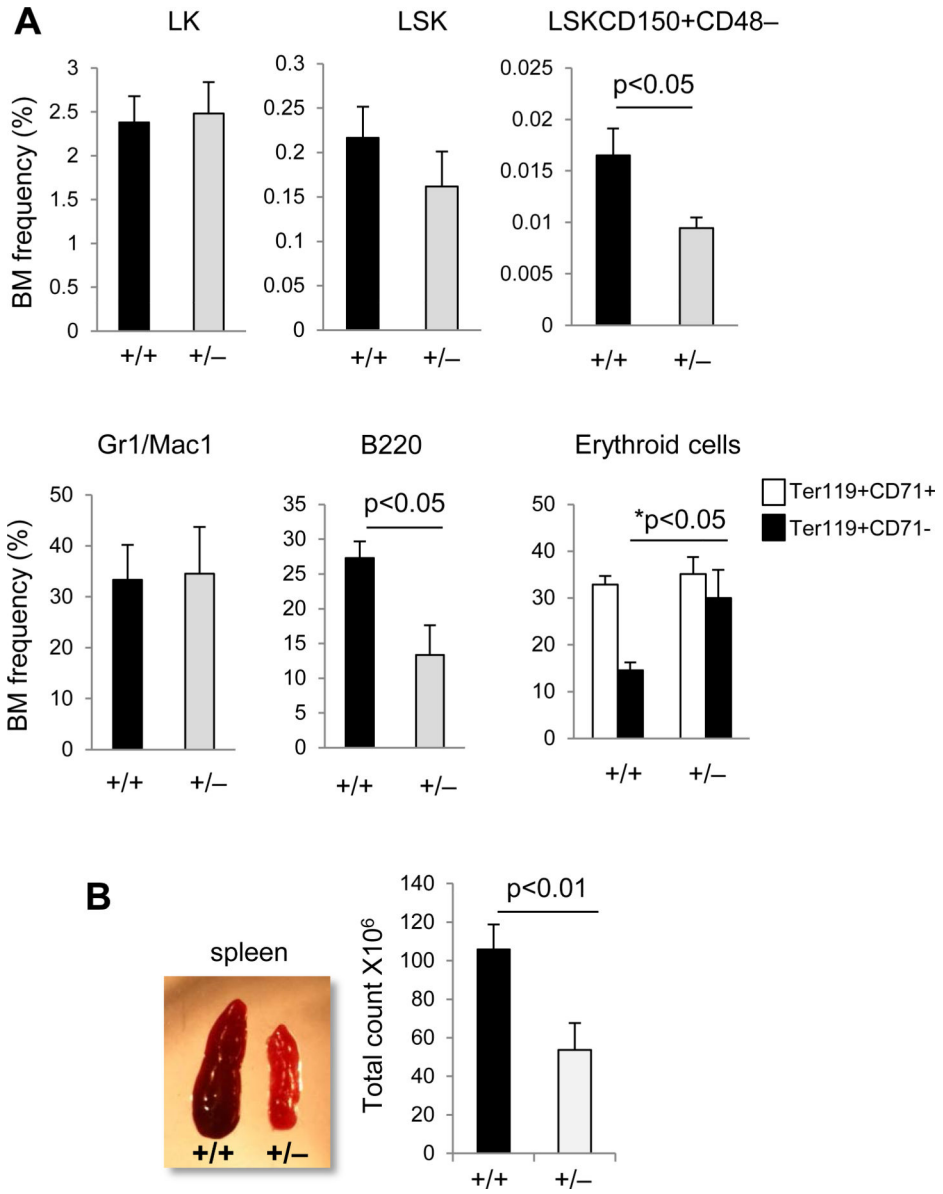

Figure 3. Hematopoietic defects in ten percent of p190-B haploinsufficient adult mice

Ten percent of p190-B haploinsufficient adult mice live shortly and develop brain hemorrhage and hematopoietic abnormalities. Hematopoietic lineages of these animals was analyzed and compared to age-matched WT controls. **(A)** Frequency of LT-HSC, progenitors (LSK and LK), granulo-monocytic cells (Gr-1+CD11b+), B cell (B220+) and erythroid lineages (Ter119+CD71+, Ter119+CD71-) in BM (mean±SD, n=8). **(B)** Images of spleen of WT and p190-B$^{+/-}$ adult mice that live shortly. Histogram is total number of cells per spleen, (mean±SD, n=5).

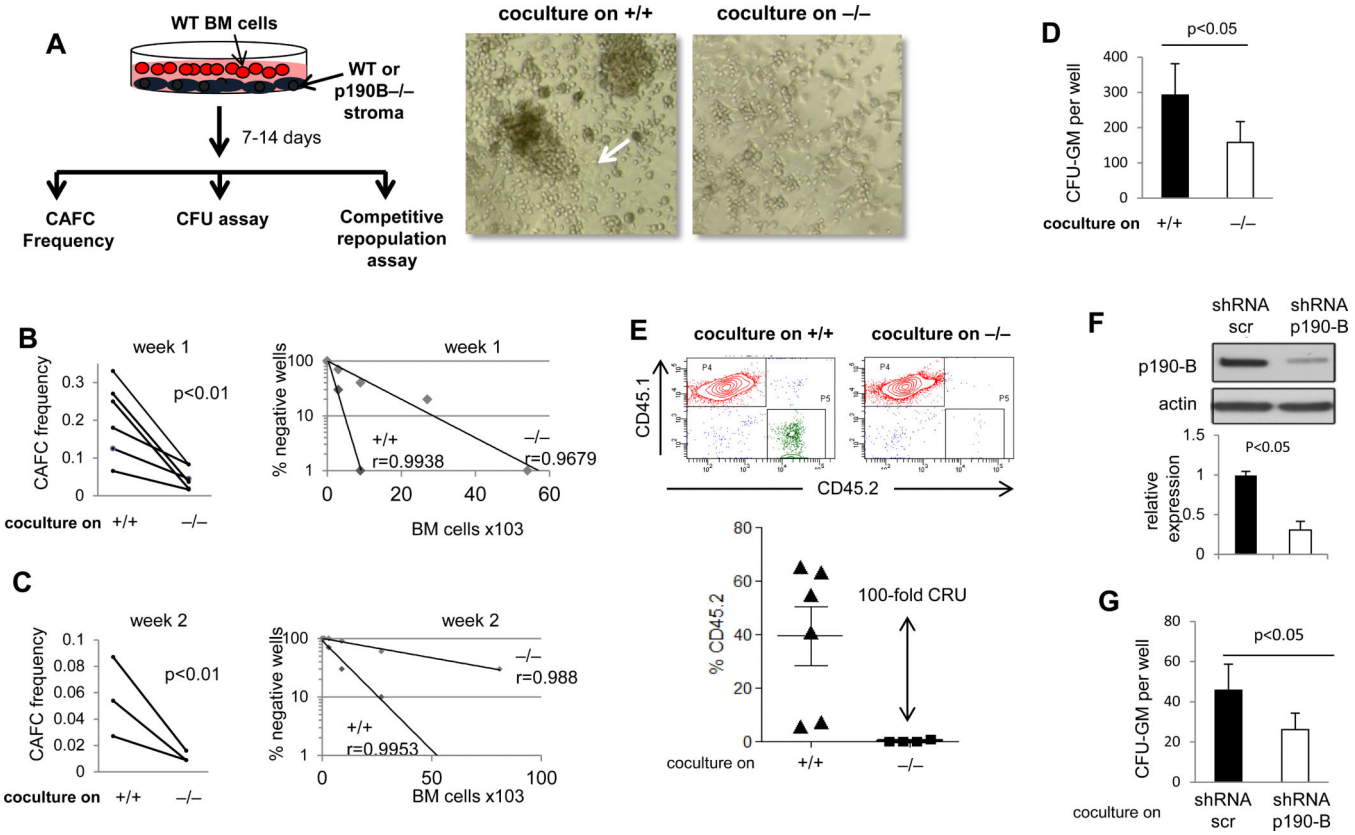

Figure 4. Defective hematopoietic supportive activity of p190-B$^{-/-}$ FL stromal cells

Coculture of WT bone marrow cells on WT and p190-B stroma in cobblestone area-forming cell (CAFC) conditions. **(A)** Schema of experiments and representative picture of cocultures taken at day 7. Arrow points to a CAFC on WT stroma. **(B&C)** CAFC frequency at week 1 (B) and week 2 (C) of co-culture. Each paired dots represents one experiment, n=5 independent experiment each performed with independently derived stroma. The right panel represents the percent of negative wells per number of bone marrow cells cocultured on each stroma. CAFC were enumerated at light microscopy; one representative experiment is shown. **(D)** Analysis of colony formation ability after one week of coculture on each stroma (mean±SD, 3 independent stroma). **(E)** Repopulation potential of hematopoietic cells following one week co-culture with each stroma, assessed by competitive repopulation assay. Representative CD45.2 and CD45.1 analysis in the peripheral blood by flow cytometry. Histogram is frequency of CD45.2 in the peripheral blood at 4 month following transplantation. mean±SD, n=6, 2 independent experiments performed with independent stromal cells. **(F)** Representative Western blot showing p190-B expression in WT MSCs after lentiviral infection with control shRNA (Scramble) or an shRNA targeting p190-B (shRNA p190-B). Actin was used as a loading control. **(G)** Numbers of CFU-GM recovered from one week coculture on WT stroma infected with ShRNA scramble or shRNA-p190-B (mean±SD, 3 lentiviral infections of independent stroma, lentiviral infection was performed in duplicate each time).

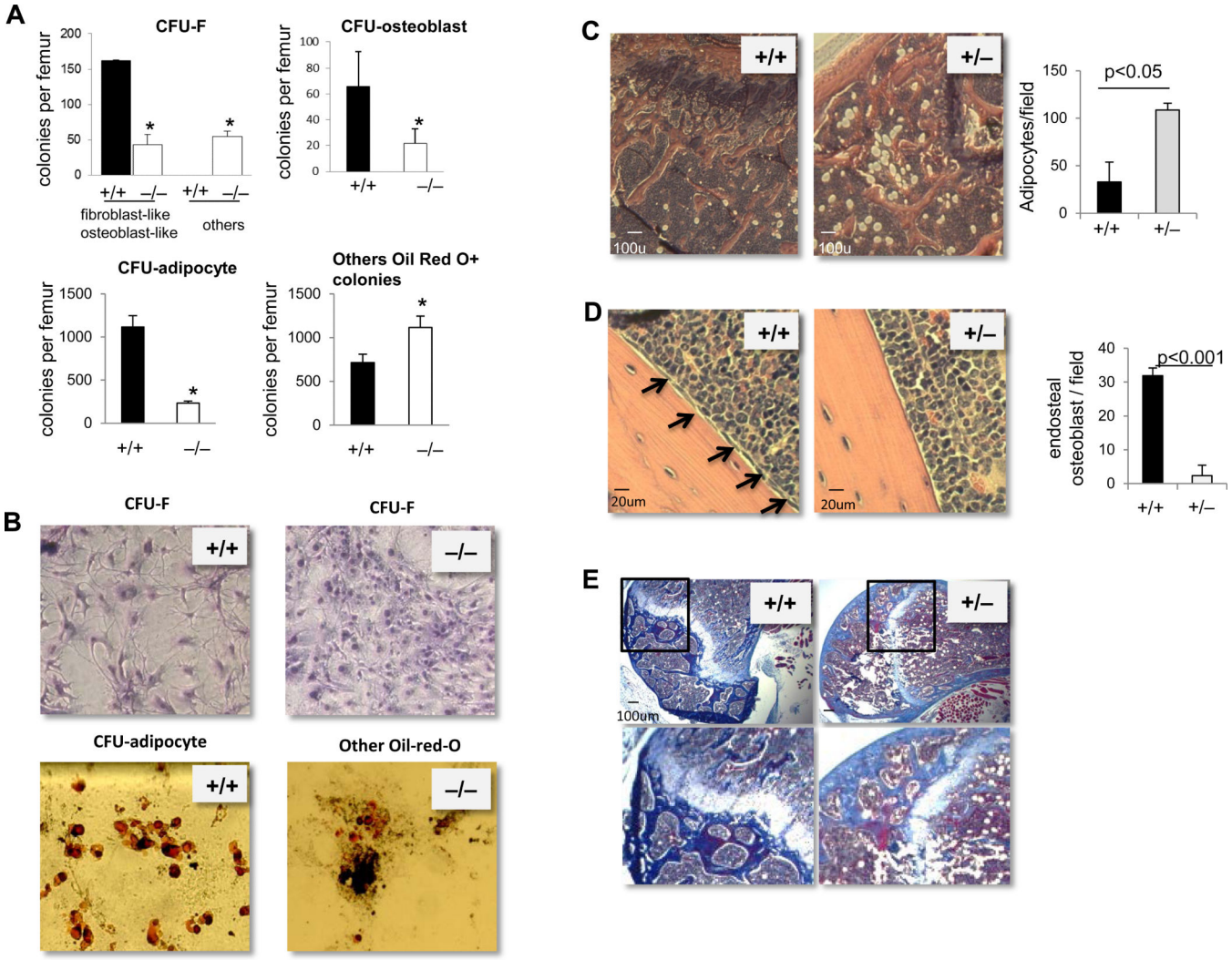

Figure 5. Mesenchymal/stromal-derived lineage defects in p190-B$^{-/-}$ FL embryos

(A) CFU-F, CFU-osteoblasts and CFU-adipocytes per femur of e18.5 WT and p190-B$^{-/-}$ embryos. (mean±SD, n=3). **(B)** Representative images of CFU-F and CFU-adipocyte colonies from each genotypes. *p<0.05. **(C&D)** Representative micrograph of decalcified longitudinal femoral section of WT and p190-B$^{+/-}$ mice stained with Haematoxylin and eosin.(C) Images show adipocytes in head of femur. Histogram is number of adipocytes per femur head (mean±SD, n=3). (D) Images show endosteal osteoblasts (black arrow). Histogram is number of endosteal osteoblasts per field (mean±SD, from 3 fields per section and in 3 independent femurs). **(E)** Masson's trichrome staining of decalcified femurs of WT and p190B$^{+/-}$ mice showing collagen deposition (in blue), representative of 3 independent femurs.

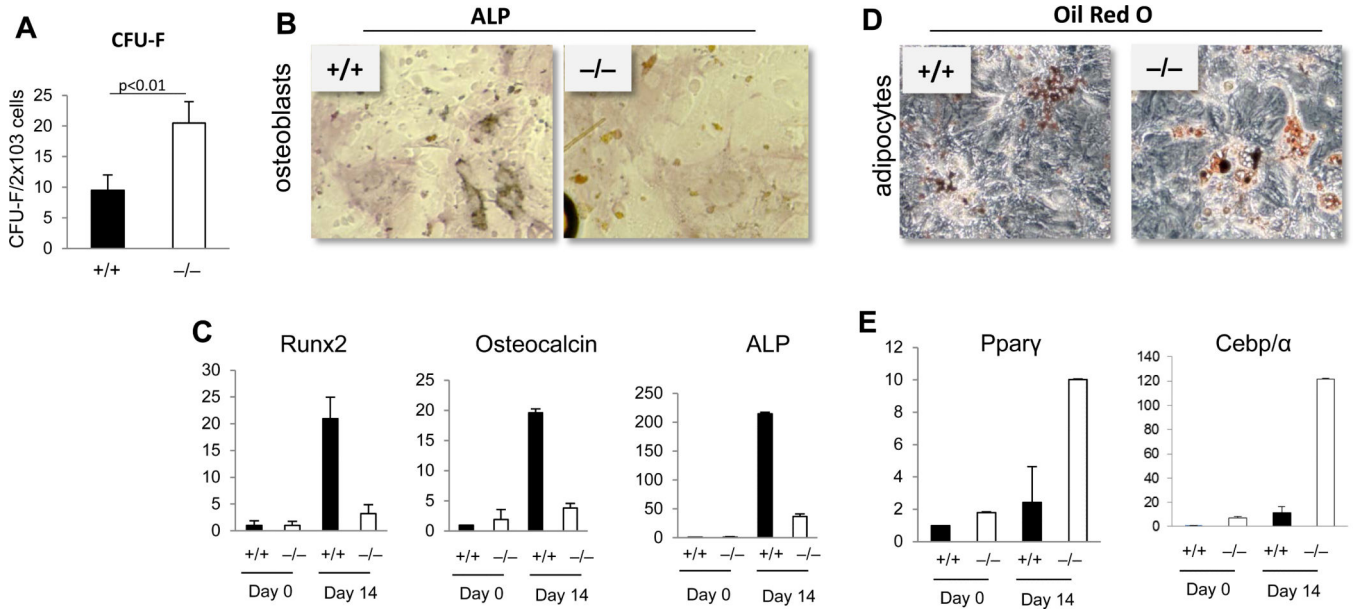

Figure 6. Characterization of p190-B-deficient FL MSCs

(A) Number of CFU-F per cultured-derived stromal cells (mean±SD, n=4). **(B)** Stromal cells were grown under osteoblastic conditions and analyzed for alkaline phosphatase staining. Representative picture of at least 3 independent cultures **(C)** qPCR analysis of the mRNA expression of osteoblastic genes before and 14 days after induction of differentiation (mean ±SD, n=3). **(D)** Stromal cells were grown under adipocytic conditions and analyzed for Oil-Red O staining. Representative picture of at least 3 independent cultures. **(E)** qPCR analysis of the mRNA expression of adipocytic genes before and 14 days after induction of differentiation (mean±SD, n=3). *p<0.05

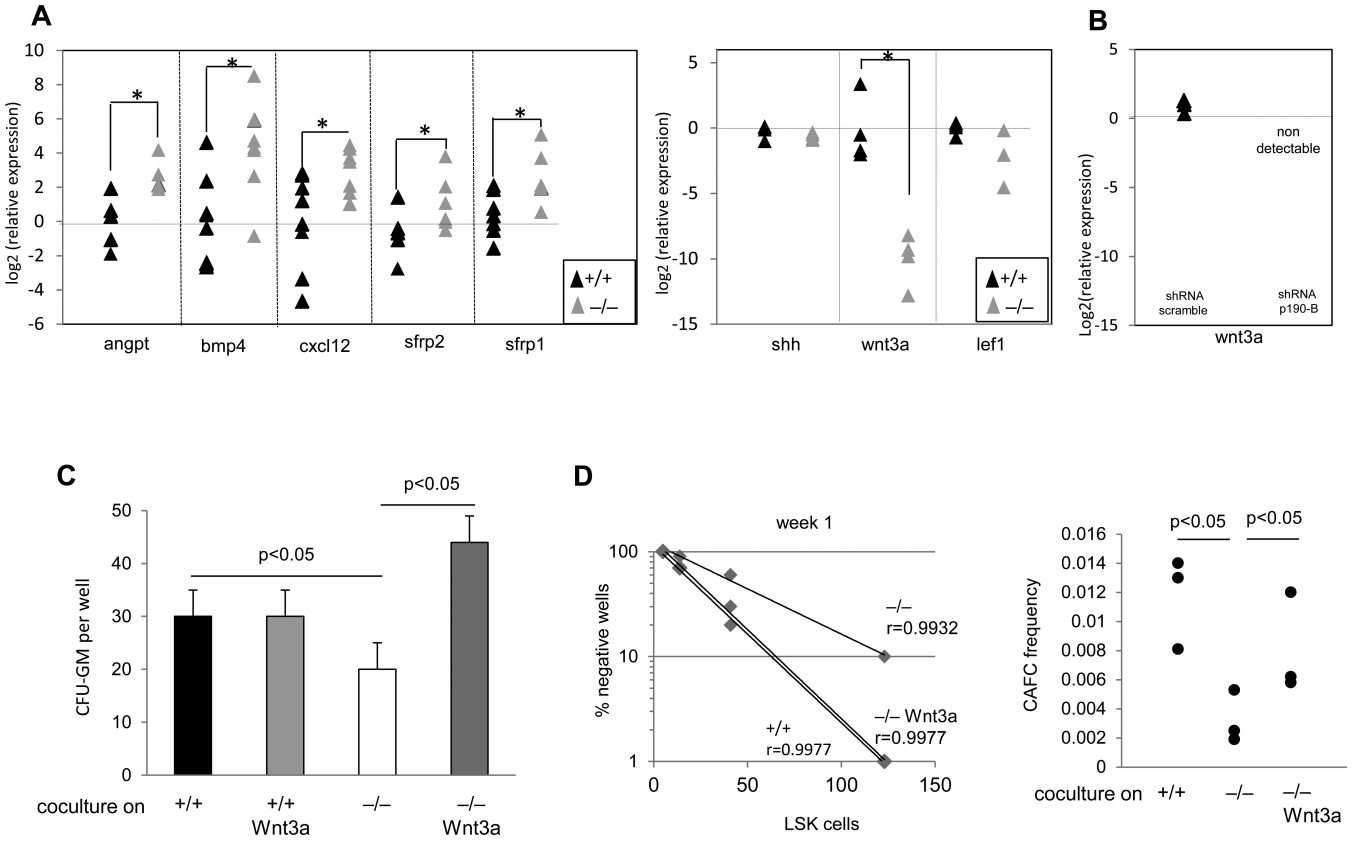

Figure 7. p190-B regulates hematopoietic supportive activity of stroma via Wnt3a

(A) qPCR analysis of the mRNA expression of various genes from independent stromal cells. Data are expressed as $\log_2$ fold relative to average of WT samples set to 0, *p<0.05 Mann-Whitney test, n=4-6 samples per group, each triangle represents one independent sample. **(B)** qPCR analysis of Wnt3a mRNA expression in WT stromal cells infected with sh-RNA scramble and shRNA-p190B, as shown in the figure 4. Log_2 fold relative to average of WT –shRNA scramble set to 0. ND: non-detectable. **(C)** Sorted LSK cells were cocultured on WT and p190B−/− stroma for one week either in presence or absence of recombinant Wnt3a. Total number of CFU-GM colonies recovered from cocultures (mean ±SD, 3 independent experiments performed with independent stroma). **(D)** CAFC frequency after one week in coculture. The right panel represents the percent of negative wells per number of cells cocultured on each stroma; one representative experiment is shown. Left panel is calculated CAFC frequency. Each dot represents one experiment, n=3 independent experiment each performed with independent stroma.